cause a decrease in the Na^+ ion concentration close to the liquid sulphur, which also agrees with earlier reported observation (Birk, 1976).

The investigation of β''-alumina by high-resolution transmission electron microscopy will continue in our laboratory and will include material used for extended periods in battery systems.

This work was supported by the Swedish Natural Science Research Council.

References

Adelsköld, V. (1938). *Ark. Kemi Mineral. Geol.* **12A** (No. 29), 1–9.

Andersson, S. & Hyde, B. (1974). *J. Solid State Chem.* **9**, 92–101.

Beevers, C. A. & Ross, M. A. S. (1937). *Z. Kristallogr.* **97**, 59–66.

Bettman, M. & Peters, K. R. (1969). *J. Phys. Chem.* **73**, 1774–1780.

Bevan, D. J. M., Hudson, B. & Moseley, P. T. (1974). *Mater. Res. Bull.* **9**, 1073–1084.

Birk, J. R. (1976). *Proc. Conf. Superionics on Superionics*, Schenectady, N.Y., pp. 1–14.

Bovin, J.-O. (1978). *Nature (London)*, **273**, 136–138.

Bragg, W. L., Gottfried, C. & West, J. (1931). *Z. Kristallogr.* **77**, 255–274.

Bursill, L. A. & Wilson, A. R. (1977). *Acta Cryst.* A**33**, 672–676.

Cowley, J. M. & Iijima, S. (1972). *Z. Naturforsch. Teil A*, **27**, 445–451.

Cowley, J. M. & Moodie, A. F. (1957). *Acta Cryst.* **10**, 609–619.

Curien, H., Guillemin, C., Orcel, J. & Sternberg, M. (1956). *C. R. Acad. Sci.* **242**, 2845–2847.

DeJonghe, L. C. (1975). *J. Mater. Sci.* **10**, 2173–2175.

DeJonghe, L. C. (1976). *J. Mater. Sci.* **11**, 206–208.

DeJonghe, L. C. (1977*a*). *J. Mater. Sci.* **12**, 497–502.

DeJonghe, L. C. (1977*b*). *Mater. Res. Bull.* **12**, 667–674.

Fejes, P. (1973). Ph.D. Thesis, Arizona State University.

Goodman, P. & Moodie, A. F. (1974). *Acta Cryst.* A**30**, 280–290.

Gratias, D., Boilot, J. P., LeCars, Y. & Théry, J. (1976). *Phys. Status Solidi A*, **38**, 595–600.

Heidenreich, R. D. (1964). *Fundamentals of Transmission Electron Microscopy*, p. 112. New York: Interscience.

Iijima, S. (1973). *Acta Cryst.* A**29**, 18–24.

LeCars, Y., Gratias, D., Portier, R. & Théry, J. (1975). *J. Solid State Chem.* **15**, 218–222.

O'Keefe, M. A. (1973). *Acta Cryst.* A**29**, 389–401.

Peters, C. R., Bettman, M., Moore, J. W. & Glick, M. D. (1971). *Acta Cryst.* B**27**, 1826–1834.

Roth, W. L. (1972). *Proc. 5th Mater. Res. Symp. NBS Spec. Publ.* 364, pp. 129–137.

Sato, S. & Hirotsu, Y. (1976). *Mater. Res. Bull.* **11**, 1307–1318.

Stevens, R. (1974). *J. Mater. Sci.* **9**, 801–808.

Stevens, R. & Miles, L. J. (1976). *J. Mater. Sci.* **11**, 1911–1918.

Van Landuyt, J., Amelinckx, S., Kohn, J. A. & Eckart, D. W. (1974). *J. Solid State Chem.* **9**, 103–119.

Yamaguchi, G. & Suzuki, K. (1968). *Bull. Chem. Soc. Jpn*, **41**, 93–99.

Acta Cryst. (1979). A**35**, 580–583

On the Structure of Mn_5Si_3, Th_6Mn_{23} and γ-Brass

By Harry Nyman and Sten Andersson

Inorganic Chemistry 2, *Chemical Center, University of Lund, PO Box* 740, *S*-220 07 *Lund, Sweden*

(*Received* 11 *December* 1978; *accepted* 18 *January* 1979)

Abstract

The structures of Mn_5Si_3, Th_6Mn_{23} and γ-brass are accurately derived from octahedra (Mn_5Si_3), tetrahedra and triangle-capping. The relationship between pyrochlore, Th_6Mn_{23} and γ-brass is also derived.

Introduction

Recently we showed how a unit of six triangles sharing edges with a central tetrahedron generated the essential part of a complex of four face-sharing icosahedra (Andersson, 1978). Searching for other applications of triangle-capping, we came across the structures of Mn_5Si_3, Th_6Mn_{23} and γ-brass, the latter two related to each other and also to the pyrochlore structure.

Mn_5Si_3

If the free edges of a chain of face-sharing octahedra are capped with triangles, the result is a column which can be used to construct the structure of Mn_5Si_3. Such columns put together over the free triangle corners, as shown in Fig. 1, make up the Mn framework of Mn_5Si_3. If we assume ideal triangles and octahedra, with unit edge e, cell dimensions can be derived:

$$a = e(\sqrt{3} + 3)/2; \quad c = e2\sqrt{2}/\sqrt{3}; \quad c/a = 0{\cdot}690.$$

The 6(g) parameter for the Mn atoms becomes

$$x = (\sqrt{3} - 1)/3 = 0{\cdot}244.$$

0567-7394/79/040580-05$01.00

Observed parameters from a recent refinement (Parthé, Jeitschko & Sadagopan, 1965) are $c/a = 0{\cdot}693$ and $x = 0{\cdot}240$.

The Si position is obtained by triangle-capping of the edges of the shared octahedral faces. Such a triangle has two shorter edges, due to the smaller Si atom and the available space of the surrounding polyhedron, which is a distorted tricapped trigonal prism.

Th_6Mn_{23}

Stella quadrangula units were used to describe parts of the structures of pyrochlore (Nyman, Andersson, Hyde & O'Keeffe, 1978) and Rh_7Mg_{44} (Andersson, 1978). Such units consist of a central tetrahedron sharing its faces with four other tetrahedra. If the outer tetrahedra of one unit share corners with outer tetrahedra of other units, the Fe part of the W_3Fe_3C structure (pyrochlore) is obtained and shown here in Fig. 2.

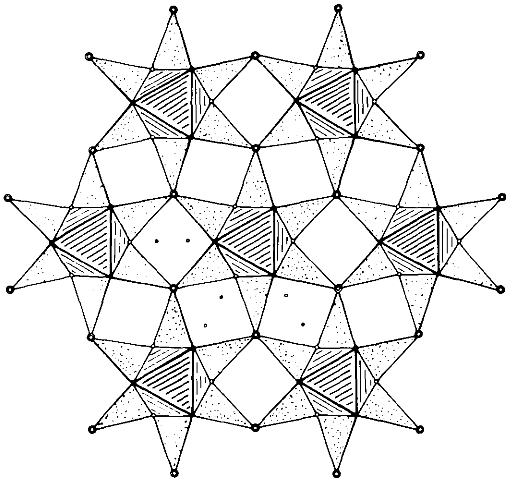

Fig. 1. The structure of Mn_5Si_3. The unconnected circles are Si atoms.

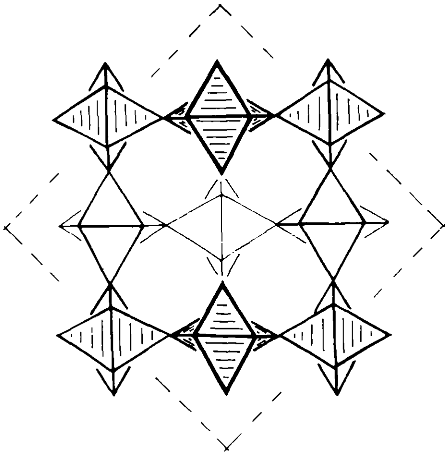

Fig. 2. The Fe structure in W_3Fe_3C.

If each edge of the central tetrahedron in the *stella quadrangula* unit is capped, a new building block is obtained, which can also be described as consisting of four interpenetrating pentagonal bipyramids. Each bipyramid consists of three regular and two irregular tetrahedra, created by the capping. In the irregular tetrahedra, one dihedral angle is 74·20° instead of 70·53°, the corresponding angle in a regular tetrahedron. By corner-sharing these blocks over the triangles, an accurate description of the Mn structure of Th_6Mn_{23} is obtained. As shown in Fig. 3, the remaining Mn atoms are situated in cubes of eight Mn atoms formed by the capped *stella quadrangula* units. The caves in the Mn skeleton are occupied by Th_6 octahedra.

This description of the structure is attractive because of its relationship to the pyrochlore structure, and also because it is precise. The calculated unit cell and coordinates are

$$a = e(\sqrt{2} + 2\sqrt{3}), \quad e \text{ is tetrahedral or triangle edge,}$$

$$\text{Mn(I) in } 32(f); \quad x = e\sqrt{2}/4a = 0{\cdot}0725,$$

$$\text{Mn(II) in } 32(f); \quad x = (e\sqrt{6}\sin\tfrac{3}{2}\,\theta)/4a = 0{\cdot}1208,$$

θ is the dihedral angle of an ideal tetrahedron. Observed parameters for the refined structure of Sr_6Mg_{23} (Wang, Kanda, Miskell & King, 1965) are 0·076 and 0·1241, with an error of ±0·0040.

γ-brass, Cu_5Zn_8

Early work describes this structure as a body-centered metal, slightly distorted and with two atoms missing in the cubic unit-cell. Bradley & Jones (1933) were the first to describe the γ-brass structure in terms of clusters, each containing 26 atoms. This description is

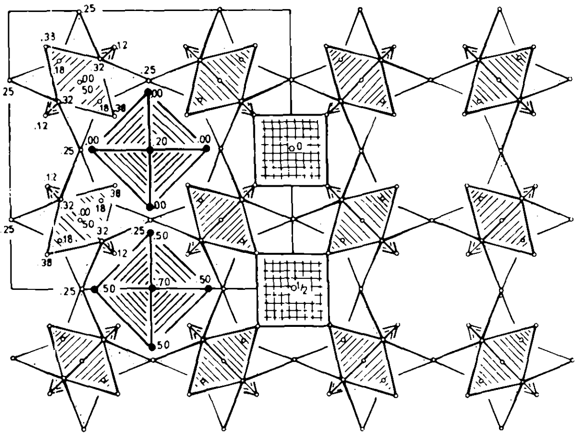

Fig. 3. Triangle-capped (dotted triangles) *stella quadrangula* form the structure of Th_6Mn_{23}. In the left part the perpendicular capping is shown with atoms at 0·00 and 0·50 forming the bridges to other *stella quadrangula*, below and above.

now commonly accepted, and one cluster consists, from the origin and outwards, of one inner tetrahedron, one outer large tetrahedron, one large octahedron, and one large irregular cube octahedron.

In our description we shall use ideal tetrahedra and ideal triangles to create the same cluster, and in that way we arrive at not only an accurate structure, but also a structure which is easily related to several others.

We start with the *stella quadrangula*, which corresponds to the outer tetrahedron above. Capping it in the Th_6Mn_{23} way gives the outer octahedron. The cluster is then completed with a triangular cap on every edge of the *stella quadrangula*, giving the distorted outer cube octahedron. The cluster is shown in Fig. 4, and a body-centered cubic arrangement of such clusters gives the structure of γ-brass.

The model structure agrees, within experimental error, with the structure of γ-brass. Cell parameter and coordinates calculated from the model are

$$a = e(\sqrt{2}/2 + \sqrt{3} + 1),$$

e is unit distance of tetrahedral or triangle edge,

$$x[12(e)] = e(\sqrt{2} + 2\sqrt{3})/4a = 0{\cdot}355,$$

$$x[8(c)] = e\sqrt{2}/4a = 0{\cdot}103,$$

$$x[8(i)] = (e\sqrt{3}\,\sin \tfrac{3}{2}\theta)/2a\sqrt{2} = 0{\cdot}171,$$

$$x[24(g)] = e[1 + 2\cos(120 - 2\arccos\sqrt{3}/3)]/2a\sqrt{2} = 0{\cdot}305,$$

$$z[24(g)] = e[\sin(120 - 2\arccos\sqrt{3}/3)]/a = 0{\cdot}053.$$

Several γ-brass structures were recently refined (Brandon, Brizard, Chieh, McMillan & Pearson, 1974) and the coordinates, averaged from three different structures, are 0·354, 0·102, 0·167, 0·305 and 0·048. The overall deviation is ~0·008 between the determinations.

Fig. 5 demonstrates the development of the structures of γ-brass from that of the *stella quadrangula* units of pyrochlore. The full body-centered arrangement of atoms is given in the left part of the figure, and in the middle the *stella quadrangula* units are capped as in Th_6Mn_{23}. The complete capping of the 26-atom cluster is shown in the right part of the figure, where the body-centered translation is left out. Fig. 6 gives a colour picture of the structure of γ-brass. The blue triangles are capping of the *stella quadrangula* as in Th_6Mn_{23}.

The result of packing atoms as close as possible, *i.e.* making ideal tetrahedra share faces, is shown in Fig. 7(*a*). Instead of using one of the two possibilities in Fig. 7(*a*), a position midway is chosen by Nature, Fig. 7(*b*). This is demonstrated by the triangle-capping concept; the blue triangles in Fig. 6 cap the *stella quadrangula* and form the building-block unit of Th_6Mn_{23}. In the final cluster every regular tetrahedron is capped by

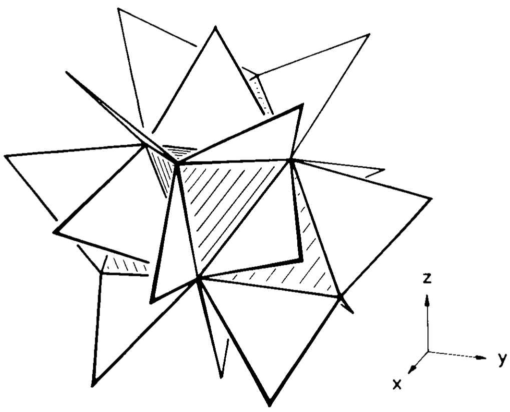

Fig. 4. A clinographic projection of the γ-brass cluster. The shaded part is the *stella quadrangula*.

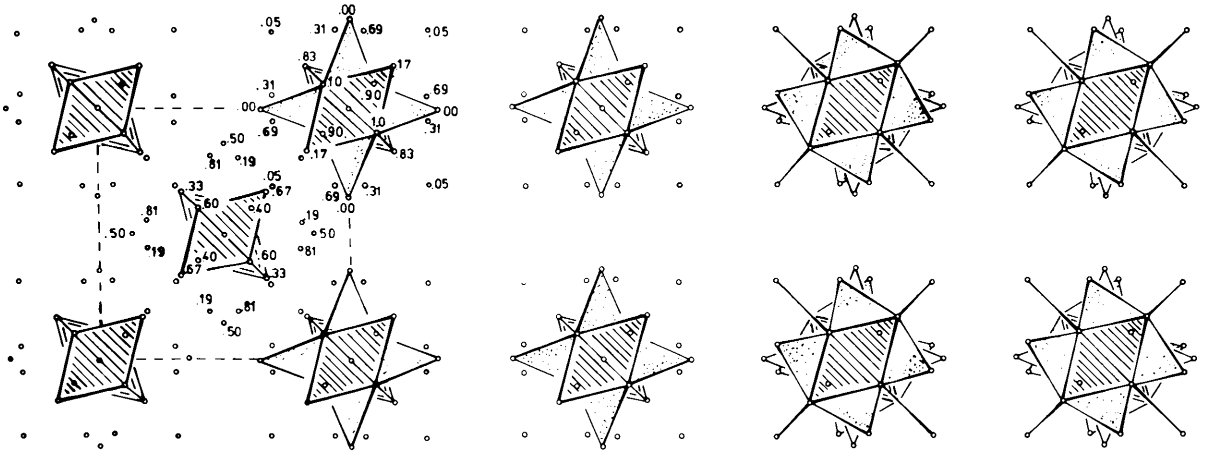

Fig. 5. The structure of γ-brass. Starting from the left it is shown how the structure can be obtained by capping *stella quadrangula* with ideal triangles

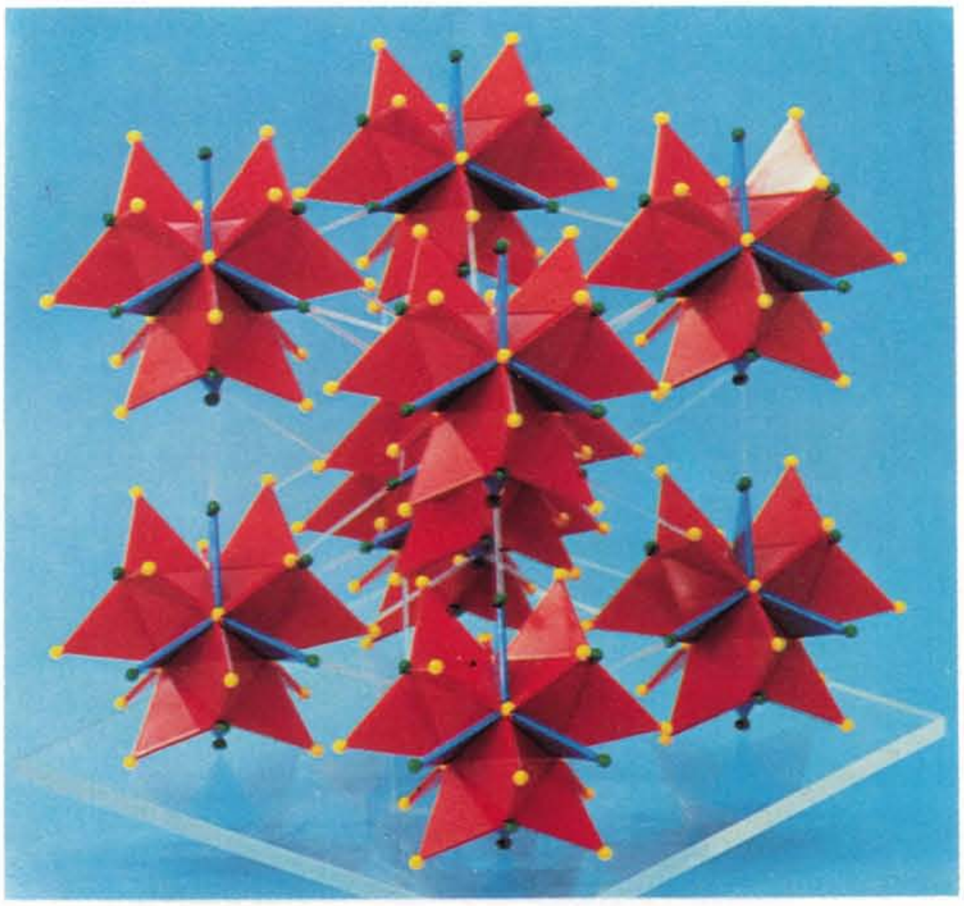

Fig. 6. Model of γ-brass. Green balls are Cu and yellow balls Zn atoms.

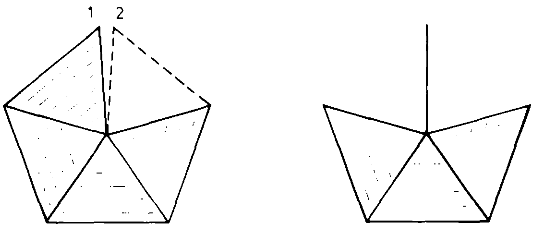

(a) (b)

Fig. 7. (*a*) The two possibilities for packing four face-sharing tetrahedra. (*b*) Nature's solution to the problem.

triangles. This could be the reason why the cluster is limited to 26 atoms; further capping gives more and more distorted tetrahedra.

This work was supported by the Swedish Natural Research Council.

References

Andersson, S. (1978). *Acta Cryst.* A**34**, 833–835.

Bradley, A. J. & Jones, P. (1933). *J. Inst. Met.* **51**, 131–158.

Brandon, J. K., Brizard, R. Y., Chieh, P. C., McMillan, R. K. & Pearson, W. B. (1974). *Acta Cryst.* B**30**, 1412–1417.

Nyman, H., Andersson, S., Hyde, B. G. & O'Keeffe, M. (1978). *J. Solid State Chem.* In the press.

Parthé, E., Jeitscko, W. & Sadagopan, V. (1965). *Acta Cryst.* **19**, 1031–1037.

Wang, F. E., Kanda, F. A., Miskell, C. F. & King, A. J. (1965). *Acta Cryst.* **18**, 24–31.

Acta Cryst. (1979). A**35**, 583–587

Diffraction-Broadening Studies of Textured Materials

By S. K. Peneva

University of Sofia 'Kliment Okhridski', Chemical Faculty, Department of Physical Chemistry, Sofia 1126, *Bulgaria*

(*Received* 4 *July* 1978; *accepted* 6 *February* 1979)

Abstract

Reciprocal-space calculations are carried out with the aim of finding out where on an electron or X-ray diffraction picture one has to measure diffraction line broadening, so as to obtain reliable information about the apparent domain size (DS) and the microstrain (MS) in a textured material. It has been shown that in both cases there are geometrical limitations. They are greater for X-ray diffraction broadening studies, and if the texture axis is arbitrarily inclined, a readjustment of the texture axis to positions parallel to the X-ray beam, or parallel to the camera axis, is required. Deviation of the texture axis from an ideal orientation increases the number of diffraction spots requiring correct correlation of their diffraction broadening with the DS and MS of the material.

Introduction

Measurements of coherent domain size (DS) and microstrain (MS) of randomly oriented and of textured polycristalline materials are expected to possess specific features, since there are differences between their corresponding reciprocal lattices. There are reliable methods for calculating DS and MS, as summarized, for example, by Lipson & Steeple (1970), but the question of where to measure diffraction line broadening in the case of textured materials remains unclear.

Kagan (1964) has pointed out some of the existing uncertainties, but his calculations are in real space and cannot be easily generalized.

A treatment in reciprocal space is carried out in the present paper, with the aim of finding out where on an electron or X-ray diffraction picture one can obtain reliable information about DS and MS of a textured material in the cases of ideal and real textures. The accent of the calculations is on electron diffraction, but the results are extended for X-ray diffraction broadening studies as well.

Essentials

The reciprocal lattice of a strained, fine grain texture is obtained by rotating around the texture axis the reciprocal lattice of a strained small single-crystal. As a first approximation, the reciprocal volume around each *hkl* lattice point is assumed to be a sphere with radius *r*.

0567-7394/79/040583-05$01.00